

SLAC-PUB-8847
August 2001
BABAR-PUB-01/06
hep-ex/0107019

Measurement of the B^0 and B^+ Meson Lifetimes with Fully Reconstructed Hadronic Final States

The *BABAR* Collaboration

Submitted to Physical Review Letters

Stanford Linear Accelerator Center, Stanford University, Stanford, CA 94309

Work supported by Department of Energy contract DE-AC03-76SF00515.

Measurement of the B^0 and B^+ meson lifetimes with fully reconstructed hadronic final states

The *BABAR* Collaboration

B. Aubert,¹ D. Boutigny,¹ J.-M. Gaillard,¹ A. Hicheur,¹ Y. Karyotakis,¹ J. P. Lees,¹ P. Robbe,¹ V. Tisserand,¹
A. Palano,² G. P. Chen,³ J. C. Chen,³ N. D. Qi,³ G. Rong,³ P. Wang,³ Y. S. Zhu,³ G. Eigen,⁴ P. L. Reinertsen,⁴
B. Stugu,⁴ B. Abbott,⁵ G. S. Abrams,⁵ A. W. Borgland,⁵ A. B. Breon,⁵ D. N. Brown,⁵ J. Button-Shafer,⁵
R. N. Cahn,⁵ A. R. Clark,⁵ M. S. Gill,⁵ A. Gritsan,⁵ Y. Groysman,⁵ R. G. Jacobsen,⁵ R. W. Kadel,⁵ J. Kadyk,⁵
L. T. Kerth,⁵ S. Kluth,⁵ Yu. G. Kolomensky,⁵ J. F. Kral,⁵ C. LeClerc,⁵ M. E. Levi,⁵ T. Liu,⁵ G. Lynch,⁵
A. B. Meyer,⁵ M. Momayezi,⁵ P. J. Oddone,⁵ A. Perazzo,⁵ M. Pripstein,⁵ N. A. Roe,⁵ A. Romosan,⁵ M. T. Ronan,⁵
V. G. Shelkov,⁵ A. V. Telnov,⁵ W. A. Wenzel,⁵ P. G. Bright-Thomas,⁶ T. J. Harrison,⁶ C. M. Hawkes,⁶
D. J. Knowles,⁶ S. W. O'Neale,⁶ R. C. Penny,⁶ A. T. Watson,⁶ N. K. Watson,⁶ T. Deppermann,⁷ K. Goetzen,⁷
H. Koch,⁷ J. Krug,⁷ M. Kunze,⁷ B. Lewandowski,⁷ K. Peters,⁷ H. Schmuecker,⁷ M. Steinke,⁷ J. C. Andress,⁸
N. R. Barlow,⁸ W. Bhimji,⁸ N. Chevalier,⁸ P. J. Clark,⁸ W. N. Cottingham,⁸ N. De Groot,⁸ N. Dyce,⁸ B. Foster,⁸
J. D. McFall,⁸ D. Wallom,⁸ F. F. Wilson,⁸ K. Abe,⁹ C. Hearty,⁹ T. S. Mattison,⁹ J. A. McKenna,⁹ D. Thiessen,⁹
S. Jolly,¹⁰ A. K. McKemey,¹⁰ J. Tinslay,¹⁰ V. E. Blinov,¹¹ A. D. Bukin,¹¹ D. A. Bukin,¹¹ A. R. Buzykaev,¹¹
V. B. Golubev,¹¹ V. N. Ivanchenko,¹¹ A. A. Korol,¹¹ E. A. Kravchenko,¹¹ A. P. Onuchin,¹¹ A. A. Salnikov,¹¹
S. I. Serednyakov,¹¹ Yu. I. Skovpen,¹¹ V. I. Telnov,¹¹ A. N. Yushkov,¹¹ D. Best,¹² A. J. Lankford,¹²
M. Mandelkern,¹² S. McMahon,¹² D. P. Stoker,¹² A. Ahsan,¹³ K. Arisaka,¹³ C. Buchanan,¹³ S. Chun,¹³
J. G. Branson,¹⁴ D. B. MacFarlane,¹⁴ S. Prell,¹⁴ Sh. Rahatlou,¹⁴ G. Raven,¹⁴ V. Sharma,¹⁴ C. Campagnari,¹⁵
B. Dahmes,¹⁵ P. A. Hart,¹⁵ N. Kuznetsova,¹⁵ S. L. Levy,¹⁵ O. Long,¹⁵ A. Lu,¹⁵ J. D. Richman,¹⁵ W. Verkerke,¹⁵
M. Witherell,¹⁵ S. Yellin,¹⁵ J. Beringer,¹⁶ D. E. Dorfan,¹⁶ A. M. Eisner,¹⁶ A. Frey,¹⁶ A. A. Grillo,¹⁶ M. Grothe,¹⁶
C. A. Heusch,¹⁶ R. P. Johnson,¹⁶ W. Kroeger,¹⁶ W. S. Lockman,¹⁶ T. Pulliam,¹⁶ H. Sadrozinski,¹⁶ T. Schalk,¹⁶
R. E. Schmitz,¹⁶ B. A. Schumm,¹⁶ A. Seiden,¹⁶ M. Turri,¹⁶ W. Walkowiak,¹⁶ D. C. Williams,¹⁶ M. G. Wilson,¹⁶
E. Chen,¹⁷ G. P. Dubois-Felsmann,¹⁷ A. Dvoretzki,¹⁷ D. G. Hitlin,¹⁷ S. Metzler,¹⁷ J. Oyang,¹⁷ F. C. Porter,¹⁷
A. Ryd,¹⁷ A. Samuel,¹⁷ M. Weaver,¹⁷ S. Yang,¹⁷ R. Y. Zhu,¹⁷ S. Devmal,¹⁸ T. L. Geld,¹⁸ S. Jayatileke,¹⁸
G. Mancinelli,¹⁸ B. T. Meadows,¹⁸ M. D. Sokoloff,¹⁸ T. Barillari,¹⁹ P. Bloom,¹⁹ M. O. Dima,¹⁹ S. Fahey,¹⁹
W. T. Ford,¹⁹ D. R. Johnson,¹⁹ U. Nauenberg,¹⁹ A. Olivas,¹⁹ H. Park,¹⁹ P. Rankin,¹⁹ J. Roy,¹⁹ S. Sen,¹⁹
J. G. Smith,¹⁹ W. C. van Hoek,¹⁹ D. L. Wagner,¹⁹ J. Blouw,²⁰ J. L. Harton,²⁰ M. Krishnamurthy,²⁰ A. Soffer,²⁰
W. H. Toki,²⁰ R. J. Wilson,²⁰ J. Zhang,²⁰ T. Brandt,²¹ J. Brose,²¹ T. Colberg,²¹ G. Dahlinger,²¹ M. Dickopp,²¹
R. S. Dubitzky,²¹ E. Maly,²¹ R. Müller-Pfefferkorn,²¹ S. Otto,²¹ K. R. Schubert,²¹ R. Schwierz,²¹ B. Spaan,²¹
L. Wilden,²¹ L. Behr,²² D. Bernard,²² G. R. Bonneaud,²² F. Brochard,²² J. Cohen-Tanugi,²² S. Ferrag,²²
E. Roussot,²² S. T'Jampens,²² C. Thiebaux,²² G. Vasileiadis,²² M. Verderi,²² A. Anjomshoaa,²³ R. Bernet,²³
A. Khan,²³ F. Muheim,²³ S. Playfer,²³ J. E. Swain,²³ M. Falbo,²⁴ C. Borean,²⁵ C. Bozzi,²⁵ S. Dittongo,²⁵
M. Folegani,²⁵ L. Piemontese,²⁵ E. Treadwell,²⁶ F. Anulli,²⁷ * R. Baldini-Ferroli,²⁷ A. Calcaterra,²⁷ R. de
Sangro,²⁷ D. Falciai,²⁷ G. Finocchiaro,²⁷ P. Patteri,²⁷ I. M. Peruzzi,²⁷ * M. Piccolo,²⁷ Y. Xie,²⁷ A. Zallo,²⁷
S. Bagnasco,²⁸ A. Buzzo,²⁸ R. Contri,²⁸ G. Crosetti,²⁸ P. Fabbriatore,²⁸ S. Farinon,²⁸ M. Lo Vetere,²⁸
M. Macri,²⁸ M. R. Monge,²⁸ R. Musenich,²⁸ M. Pallavicini,²⁸ R. Parodi,²⁸ S. Passaggio,²⁸ F. C. Pastore,²⁸
C. Patrignani,²⁸ M. G. Pia,²⁸ C. Priano,²⁸ E. Robutti,²⁸ A. Santroni,²⁸ M. Morii,²⁹ R. Bartoldus,³⁰ T. Dignan,³⁰
R. Hamilton,³⁰ U. Mallik,³⁰ J. Cochran,³¹ H. B. Crawley,³¹ P.-A. Fischer,³¹ J. Lamsa,³¹ W. T. Meyer,³¹
E. I. Rosenberg,³¹ M. Benkebil,³² G. Grosdidier,³² C. Hast,³² A. Höcker,³² H. M. Lacker,³² V. LePeltier,³²
A. M. Lutz,³² S. Plaszczynski,³² M. H. Schune,³² S. Trincaz-Duvoid,³² A. Valassi,³² G. Wormser,³² R. M. Bionta,³³
V. Brigljević,³³ D. J. Lange,³³ M. Mugge,³³ X. Shi,³³ K. van Bibber,³³ T. J. Wenaus,³³ D. M. Wright,³³
C. R. Wuest,³³ M. Carroll,³⁴ J. R. Fry,³⁴ E. Gabathuler,³⁴ R. Gamet,³⁴ M. George,³⁴ M. Kay,³⁴ D. J. Payne,³⁴

R. J. Sloane,³⁴ C. Touramanis,³⁴ M. L. Aspinwall,³⁵ D. A. Bowerman,³⁵ P. D. Dauncey,³⁵ U. Egede,³⁵ I. Eschrich,³⁵ N. J. W. Gunawardane,³⁵ J. A. Nash,³⁵ P. Sanders,³⁵ D. Smith,³⁵ D. E. Azzopardi,³⁶ J. J. Back,³⁶ P. Dixon,³⁶ P. F. Harrison,³⁶ R. J. L. Potter,³⁶ H. W. Shorthouse,³⁶ P. Strother,³⁶ P. B. Vidal,³⁶ M. I. Williams,³⁶ G. Cowan,³⁷ S. George,³⁷ M. G. Green,³⁷ A. Kurup,³⁷ C. E. Marker,³⁷ P. McGrath,³⁷ T. R. McMahon,³⁷ S. Ricciardi,³⁷ F. Salvatore,³⁷ I. Scott,³⁷ G. Vaitsas,³⁷ D. Brown,³⁸ C. L. Davis,³⁸ J. Allison,³⁹ R. J. Barlow,³⁹ J. T. Boyd,³⁹ A. C. Forti,³⁹ J. Fullwood,³⁹ F. Jackson,³⁹ G. D. Lafferty,³⁹ N. Savvas,³⁹ E. T. Simopoulos,³⁹ J. H. Weatherall,³⁹ A. Farbin,⁴⁰ A. Jawahery,⁴⁰ V. Lillard,⁴⁰ J. Olsen,⁴⁰ D. A. Roberts,⁴⁰ J. R. Schieck,⁴⁰ G. Blaylock,⁴¹ C. Dallapiccola,⁴¹ K. T. Flood,⁴¹ S. S. Hertzbach,⁴¹ R. Kofler,⁴¹ T. B. Moore,⁴¹ H. Staengle,⁴¹ S. Willocq,⁴¹ B. Brau,⁴² R. Cowan,⁴² G. Sciolla,⁴² F. Taylor,⁴² R. K. Yamamoto,⁴² M. Milek,⁴³ P. M. Patel,⁴³ J. Trischuk,⁴³ F. Lanni,⁴⁴ F. Palombo,⁴⁴ J. M. Bauer,⁴⁵ M. Booke,⁴⁵ L. Cremaldi,⁴⁵ V. Eschenburg,⁴⁵ R. Kroeger,⁴⁵ J. Reidy,⁴⁵ D. A. Sanders,⁴⁵ D. J. Summers,⁴⁵ J. P. Martin,⁴⁶ J. Y. Nief,⁴⁶ R. Seitz,⁴⁶ P. Taras,⁴⁶ A. Woch,⁴⁶ V. Zacek,⁴⁶ H. Nicholson,⁴⁷ C. S. Sutton,⁴⁷ C. Cartaro,⁴⁸ N. Cavallo,⁴⁸ † G. De Nardo,⁴⁸ F. Fabozzi,⁴⁸ C. Gatto,⁴⁸ L. Lista,⁴⁸ P. Paolucci,⁴⁸ D. Piccolo,⁴⁸ C. Sciacca,⁴⁸ J. M. LoSecco,⁴⁹ J. R. G. Alsmiller,⁵⁰ T. A. Gabriel,⁵⁰ T. Handler,⁵⁰ J. Brau,⁵¹ R. Frey,⁵¹ M. Iwasaki,⁵¹ N. B. Sinev,⁵¹ D. Strom,⁵¹ F. Colecchia,⁵² F. Dal Corso,⁵² A. Dorigo,⁵² F. Galeazzi,⁵² M. Margoni,⁵² G. Michelon,⁵² M. Morandin,⁵² M. Posocco,⁵² M. Rotondo,⁵² F. Simonetto,⁵² R. Stroili,⁵² E. Torassa,⁵² C. Voci,⁵² M. Benayoun,⁵³ H. Briand,⁵³ J. Chauveau,⁵³ P. David,⁵³ C. De la Vaissière,⁵³ L. Del Buono,⁵³ O. Hamon,⁵³ F. Le Diberder,⁵³ Ph. Leruste,⁵³ J. Lory,⁵³ L. Roos,⁵³ J. Stark,⁵³ S. Versillé,⁵³ P. F. Manfredi,⁵⁴ V. Re,⁵⁴ V. Speziali,⁵⁴ E. D. Frank,⁵⁵ L. Gladney,⁵⁵ Q. H. Guo,⁵⁵ J. H. Panetta,⁵⁵ C. Angelini,⁵⁶ G. Batignani,⁵⁶ S. Bettarini,⁵⁶ M. Bondioli,⁵⁶ M. Carpinelli,⁵⁶ F. Forti,⁵⁶ M. A. Giorgi,⁵⁶ A. Lusiani,⁵⁶ F. Martinez-Vidal,⁵⁶ M. Morganti,⁵⁶ N. Neri,⁵⁶ E. Paoloni,⁵⁶ M. Rama,⁵⁶ G. Rizzo,⁵⁶ F. Sandrelli,⁵⁶ G. Simi,⁵⁶ G. Triggiani,⁵⁶ J. Walsh,⁵⁶ M. Haire,⁵⁷ D. Judd,⁵⁷ K. Paick,⁵⁷ L. Turnbull,⁵⁷ D. E. Wagoner,⁵⁷ J. Albert,⁵⁸ C. Bula,⁵⁸ P. Elmer,⁵⁸ C. Lu,⁵⁸ K. T. McDonald,⁵⁸ V. Miftakov,⁵⁸ S. F. Schaffner,⁵⁸ A. J. S. Smith,⁵⁸ A. Tumanov,⁵⁸ E. W. Varnes,⁵⁸ G. Cavoto,⁵⁹ D. del Re,⁵⁹ R. Faccini,^{14,59} F. Ferrarotto,⁵⁹ F. Ferroni,⁵⁹ K. Fratini,⁵⁹ E. Lamanna,⁵⁹ E. Leonardi,⁵⁹ M. A. Mazzone,⁵⁹ S. Morganti,⁵⁹ G. Piredda,⁵⁹ F. Safai Tehrani,⁵⁹ M. Serra,⁵⁹ C. Voena,⁵⁹ S. Christ,⁶⁰ R. Waldi,⁶⁰ P. F. Jacques,⁶¹ M. Kalelkar,⁶¹ R. J. Plano,⁶¹ T. Adye,⁶² B. Franek,⁶² N. I. Geddes,⁶² G. P. Gopal,⁶² S. M. Xella,⁶² R. Aleksan,⁶³ G. De Domenico,⁶³ S. Emery,⁶³ A. Gaidot,⁶³ S. F. Ganzhur,⁶³ G. Hamel de Monchenault,⁶³ W. Kozanecki,⁶³ M. Langer,⁶³ G. W. London,⁶³ B. Mayer,⁶³ B. Serfass,⁶³ G. Vasseur,⁶³ C. Yeche,⁶³ M. Zito,⁶³ N. Copty,⁶⁴ M. V. Purohit,⁶⁴ H. Singh,⁶⁴ F. X. Yumiceva,⁶⁴ I. Adam,⁶⁵ P. L. Anthony,⁶⁵ D. Aston,⁶⁵ K. Baird,⁶⁵ E. Bloom,⁶⁵ A. M. Boyarski,⁶⁵ F. Bulos,⁶⁵ G. Calderini,⁶⁵ R. Claus,⁶⁵ M. R. Convery,⁶⁵ D. P. Coupal,⁶⁵ D. H. Coward,⁶⁵ J. Dorfan,⁶⁵ M. Doser,⁶⁵ W. Dunwoodie,⁶⁵ R. C. Field,⁶⁵ T. Glanzman,⁶⁵ G. L. Godfrey,⁶⁵ S. J. Gowdy,⁶⁵ P. Grosso,⁶⁵ T. Himel,⁶⁵ M. E. Huffer,⁶⁵ W. R. Innes,⁶⁵ C. P. Jessop,⁶⁵ M. H. Kelsey,⁶⁵ P. Kim,⁶⁵ M. L. Kocian,⁶⁵ U. Langenegger,⁶⁵ D. W. G. S. Leith,⁶⁵ S. Luitz,⁶⁵ V. Luth,⁶⁵ H. L. Lynch,⁶⁵ H. Marsiske,⁶⁵ S. Menke,⁶⁵ R. Messner,⁶⁵ K. C. Moffeit,⁶⁵ R. Mount,⁶⁵ D. R. Muller,⁶⁵ C. P. O'Grady,⁶⁵ M. Perl,⁶⁵ S. Petrak,⁶⁵ H. Quinn,⁶⁵ B. N. Ratcliff,⁶⁵ S. H. Robertson,⁶⁵ L. S. Rochester,⁶⁵ A. Roodman,⁶⁵ T. Schietinger,⁶⁵ R. H. Schindler,⁶⁵ J. Schwiening,⁶⁵ V. V. Serbo,⁶⁵ A. Snyder,⁶⁵ A. Soha,⁶⁵ S. M. Spanier,⁶⁵ J. Stelzer,⁶⁵ D. Su,⁶⁵ M. K. Sullivan,⁶⁵ H. A. Tanaka,⁶⁵ J. Va'vra,⁶⁵ S. R. Wagner,⁶⁵ A. J. R. Weinstein,⁶⁵ W. J. Wisniewski,⁶⁵ D. H. Wright,⁶⁵ C. C. Young,⁶⁵ P. R. Burchat,⁶⁶ C. H. Cheng,⁶⁶ D. Kirkby,⁶⁶ T. I. Meyer,⁶⁶ C. Roat,⁶⁶ R. Henderson,⁶⁷ W. Bugg,⁶⁸ H. Cohn,⁶⁸ A. W. Weidemann,⁶⁸ J. M. Izen,⁶⁹ I. Kitayama,⁶⁹ X. C. Lou,⁶⁹ M. Turcotte,⁶⁹ F. Bianchi,⁷⁰ M. Bona,⁷⁰ B. Di Girolamo,⁷⁰ D. Gamba,⁷⁰ A. Smol,⁷⁰ D. Zanin,⁷⁰ L. Lanceri,⁷¹ A. Pompili,⁷¹ G. Vuagnin,⁷¹ R. S. Panvini,⁷² C. M. Brown,⁷³ A. De Silva,⁷³ R. Kowalewski,⁷³ J. M. Roney,⁷³ H. R. Band,⁷⁴ E. Charles,⁷⁴ S. Dasu,⁷⁴ F. Di Lodovico,⁷⁴ A. M. Eichenbaum,⁷⁴ H. Hu,⁷⁴ J. R. Johnson,⁷⁴ R. Liu,⁷⁴ J. Nielsen,⁷⁴ Y. Pan,⁷⁴ R. Prepost,⁷⁴ I. J. Scott,⁷⁴ S. J. Sekula,⁷⁴ J. H. von Wimmersperg-Toeller,⁷⁴ S. L. Wu,⁷⁴ Z. Yu,⁷⁴ H. Zobernig,⁷⁴ T. M. B. Kordich,⁷⁵ and H. Neal⁷⁵

¹Laboratoire de Physique des Particules, F-74941 Annecy-le-Vieux, France

²Università di Bari, Dipartimento di Fisica and INFN, I-70126 Bari, Italy

³Institute of High Energy Physics, Beijing 100039, China

⁴University of Bergen, Inst. of Physics, N-5007 Bergen, Norway

⁵Lawrence Berkeley National Laboratory and University of California, Berkeley, CA 94720, USA

⁶University of Birmingham, Birmingham, B15 2TT, United Kingdom

⁷Ruhr Universität Bochum, Institut für Experimentalphysik 1, D-44780 Bochum, Germany

⁸University of Bristol, Bristol BS8 1TL, United Kingdom

⁹University of British Columbia, Vancouver, BC, Canada V6T 1Z1

¹⁰Brunel University, Uxbridge, Middlesex UB8 3PH, United Kingdom

- ¹¹*Budker Institute of Nuclear Physics, Novosibirsk 630090, Russia*
¹²*University of California at Irvine, Irvine, CA 92697, USA*
¹³*University of California at Los Angeles, Los Angeles, CA 90024, USA*
¹⁴*University of California at San Diego, La Jolla, CA 92093, USA*
¹⁵*University of California at Santa Barbara, Santa Barbara, CA 93106, USA*
¹⁶*University of California at Santa Cruz, Institute for Particle Physics, Santa Cruz, CA 95064, USA*
¹⁷*California Institute of Technology, Pasadena, CA 91125, USA*
¹⁸*University of Cincinnati, Cincinnati, OH 45221, USA*
¹⁹*University of Colorado, Boulder, CO 80309, USA*
²⁰*Colorado State University, Fort Collins, CO 80523, USA*
²¹*Technische Universität Dresden, Institut für Kern- und Teilchenphysik, D-01062, Dresden, Germany*
²²*Ecole Polytechnique, F-91128 Palaiseau, France*
²³*University of Edinburgh, Edinburgh EH9 3JZ, United Kingdom*
²⁴*Elon College, Elon College, NC 27244-2010, USA*
²⁵*Università di Ferrara, Dipartimento di Fisica and INFN, I-44100 Ferrara, Italy I-44100 Ferrara, Italy*
²⁶*Florida A&M University, Tallahassee, FL 32307, USA*
²⁷*Laboratori Nazionali di Frascati dell'INFN, I-00044 Frascati, Italy*
²⁸*Università di Genova, Dipartimento di Fisica and INFN, I-16146 Genova, Italy*
²⁹*Harvard University, Cambridge, MA 02138, USA*
³⁰*University of Iowa, Iowa City, IA 52242, USA*
³¹*Iowa State University, Ames, IA 50011-3160, USA*
³²*Laboratoire de l'Accélérateur Linéaire, F-91898 Orsay, France*
³³*Lawrence Livermore National Laboratory, Livermore, CA 94550, USA*
³⁴*University of Liverpool, Liverpool L69 3BX, United Kingdom*
³⁵*University of London, Imperial College, London, SW7 2BW, United Kingdom*
³⁶*Queen Mary, University of London, E1 4NS, United Kingdom*
³⁷*University of London, Royal Holloway and Bedford New College, Egham, Surrey TW20 0EX, United Kingdom*
³⁸*University of Louisville, Louisville, KY 40292, USA*
³⁹*University of Manchester, Manchester M13 9PL, United Kingdom*
⁴⁰*University of Maryland, College Park, MD 20742, USA*
⁴¹*University of Massachusetts, Amherst, MA 01003, USA*
⁴²*Massachusetts Institute of Technology, Lab for Nuclear Science, Cambridge, MA 02139, USA*
⁴³*McGill University, Montréal, Canada QC H3A 2T8*
⁴⁴*Università di Milano, Dipartimento di Fisica and INFN, I-20133 Milano, Italy*
⁴⁵*University of Mississippi, University, MS 38677, USA*
⁴⁶*Université de Montréal, Lab. Rene J. A. Levesque, Montréal, Canada QC H3C 3J7*
⁴⁷*Mount Holyoke College, South Hadley, MA 01075, USA*
⁴⁸*Università di Napoli Federico II, Dipartimento di Scienze Fisiche and INFN, I-80126, Napoli, Italy*
⁴⁹*University of Notre Dame, Notre Dame, IN 46556, USA*
⁵⁰*Oak Ridge National Laboratory, Oak Ridge, TN 37831, USA*
⁵¹*University of Oregon, Eugene, OR 97403, USA*
⁵²*Università di Padova, Dipartimento di Fisica and INFN, I-35131 Padova, Italy*
⁵³*Universités Paris VI et VII, LPNHE, F-75252 Paris, France*
⁵⁴*Università di Pavia, Dipartimento di Elettronica and INFN, I-27100 Pavia, Italy*
⁵⁵*University of Pennsylvania, Philadelphia, PA 19104, USA*
⁵⁶*Università di Pisa, Scuola Normale Superiore and INFN, I-56010 Pisa, Italy*
⁵⁷*Prairie View A&M University, Prairie View, TX 77446, USA*
⁵⁸*Princeton University, Princeton, NJ 08544, USA*
⁵⁹*Università di Roma La Sapienza, Dipartimento di Fisica and INFN, I-00185 Roma, Italy*
⁶⁰*Universität Rostock, D-18051 Rostock, Germany*
⁶¹*Rutgers University, New Brunswick, NJ 08903, USA*
⁶²*Rutherford Appleton Laboratory, Chilton, Didcot, Oxon, OX11 0QX, United Kingdom*
⁶³*DAPNIA, Commissariat à l'Energie Atomique/Saclay, F-91191 Gif-sur-Yvette, France*
⁶⁴*University of South Carolina, Columbia, SC 29208, USA*
⁶⁵*Stanford Linear Accelerator Center, Stanford, CA 94309, USA*
⁶⁶*Stanford University, Stanford, CA 94305-4060, USA*
⁶⁷*TRIUMF, Vancouver, BC, Canada V6T 2A3*
⁶⁸*University of Tennessee, Knoxville, TN 37996, USA*
⁶⁹*University of Texas at Dallas, Richardson, TX 75083, USA*
⁷⁰*Università di Torino, Dipartimento di Fisica Sperimentale and INFN, I-10125 Torino, Italy*
⁷¹*Università di Trieste, Dipartimento di Fisica and INFN, I-34127 Trieste, Italy*
⁷²*Vanderbilt University, Nashville, TN 37235, USA*
⁷³*University of Victoria, Victoria, BC, Canada V8W 3P6*
⁷⁴*University of Wisconsin, Madison, WI 53706, USA*

⁷⁵Yale University, New Haven, CT 06511, USA

(Dated: July 9, 2001)

The B^0 and B^+ meson lifetimes have been measured in e^+e^- annihilation data collected in 1999 and 2000 with the *BABAR* detector at center-of-mass energies near the $\Upsilon(4S)$ resonance. Events are selected in which one B meson is fully reconstructed in a hadronic final state while the second B meson is reconstructed inclusively. A combined fit to the B^0 and the B^+ decay time difference distributions yields $\tau_{B^0} = 1.546 \pm 0.032$ (stat) ± 0.022 (syst) ps, $\tau_{B^+} = 1.673 \pm 0.032$ (stat) ± 0.023 (syst) ps and $\tau_{B^+}/\tau_{B^0} = 1.082 \pm 0.026$ (stat) ± 0.012 (syst).

PACS numbers: 13.25.Hw, 12.39.Hg

The spectator quark model predicts that the two charge states of a meson with one heavy quark Q ($Q\bar{u}$ and $Q\bar{d}$) have the same lifetime. Deviations from this simple picture are expected to be proportional to $1/m_Q^2$ [1, 2]. Therefore, any lifetime differences are anticipated to be much smaller for bottom than for charm mesons. Various models [1, 2] predict the ratio of the B^+ and B^0 meson [3] lifetimes to differ by up to 10% from unity. At present, this ratio is measured to be $\tau_{B^+}/\tau_{B^0} = 1.062 \pm 0.029$ [4], with the most precise values obtained by experiments operating near the Z and at hadron colliders.

The lifetime measurements described here are based on a sample of approximately 23 million $B\bar{B}$ pairs recorded near the $\Upsilon(4S)$ resonance with the *BABAR* detector at the Stanford Linear Accelerator Center. The PEP-II asymmetric-energy e^+e^- collider produces B^+B^- and $B^0\bar{B}^0$ pairs moving along the beam axis (z direction) with a nominal Lorentz boost of $\beta\gamma = 0.56$. Hence, on average, the two B decay vertices are separated by $\langle|\Delta z|\rangle = \beta\gamma\gamma_B^{\text{cms}}c\tau \approx 270\ \mu\text{m}$, where τ is either the B^0 or B^+ lifetime, and γ_B^{cms} is the Lorentz factor of the B mesons in the $\Upsilon(4S)$ rest frame. This separation allows B lifetimes to be measured at the $\Upsilon(4S)$, with good statistical precision and systematic error sources different from those in previously published results.

In this analysis, one of the B mesons in an event, denoted B_{rec} , is fully reconstructed in a variety of two-body charm and charmonium final states. The decay point of the other B in the event, B_{opp} , is reconstructed inclusively. The decay probability distribution is given by

$$g(\Delta t|\tau) = \frac{1}{N} \cdot \frac{dN}{d(\Delta t)} = \frac{1}{2\tau} e^{-|\Delta t|/\tau}, \quad (1)$$

where $\Delta t = t_{\text{rec}} - t_{\text{opp}}$ is the (signed) difference of the proper decay times of the B mesons. The time interval Δt between the two B decays is determined from Δz , including an event-by-event correction for the direction of the B mesons with respect to the z direction in the $\Upsilon(4S)$ frame. The challenge of the measurement is to disentangle the resolution in Δz , $190\ \mu\text{m}$ on average, from the effects of the B lifetime, since both contribute to the width of the Δt distribution. In the absence of background, the measured Δt distribution is described by the

probability density function (PDF)

$$\mathcal{G}(\Delta t, \sigma|\tau, \hat{a}) = \int_{-\infty}^{+\infty} g(\Delta t'|\tau) \mathcal{R}(\Delta t - \Delta t', \sigma|\hat{a}) d(\Delta t'), \quad (2)$$

where \mathcal{R} is the Δt resolution function with parameters \hat{a} , and σ is the event-by-event error on Δt calculated from the vertex fits. An unbinned maximum likelihood fit is used to extract the B^0 and B^+ lifetimes from the Δt distributions for $B^0\bar{B}^0$ and B^+B^- events.

The *BABAR* detector is described in detail elsewhere [5]. Charged particle trajectories are measured by a combination of a silicon vertex tracker (SVT) and a drift chamber (DCH) in a 1.5-T solenoidal field. For 1 GeV/ c tracks, the impact parameter resolutions in z and in the transverse plane are $65\ \mu\text{m}$ and $55\ \mu\text{m}$, respectively. Photons and electrons are detected in the CsI(Tl) electromagnetic calorimeter (EMC). A ring imaging Cherenkov detector, the DIRC, is used for charged hadron identification. The DCH and SVT also provide ionization measurements, dE/dx , for particle identification. The instrumented flux return (IFR) is segmented and contains resistive plate chambers to identify muons. Electron candidates are required to have a ratio of EMC energy to track momentum, an EMC cluster shape, DCH dE/dx and DIRC Cherenkov angle consistent with the electron hypothesis. Muon candidates are required to have an energy deposit in the EMC consistent with the muon hypothesis, IFR hits located consistently on the extrapolated DCH track, and an IFR penetration in interaction lengths consistent with the muon hypothesis.

B^0 and B^+ mesons are reconstructed in a sample of multihadron events in the modes $B^0 \rightarrow D^{(*)-}\pi^+$, $D^{(*)-}\rho^+$, $D^{(*)-}a_1^+$, $J/\psi K^{*0}$ and $B^+ \rightarrow \bar{D}^{(*)0}\pi^+$, $J/\psi K^+$, $\psi(2S)K^+$. Multihadron events must have a minimum of three reconstructed charged tracks, a total charged and neutral energy greater than 4.5 GeV, and an event vertex within 0.5 cm of the beam spot [5] center in xy and within 6 cm in z . The event vertex is determined from all charged tracks that have an impact parameter with respect to the beam spot center smaller than 1 cm in xy and 3 cm in z .

For π^0 candidates, pairs of photons in the EMC, each with more than 30 MeV of energy, are selected if their

invariant mass is within $20 \text{ MeV}/c^2$ of the π^0 mass [4] and their total energy exceeds 200 MeV (100 MeV for the soft π^0 in D^* decays). A mass constraint is applied to selected candidates for use in the subsequent reconstruction chain.

$K_s^0 \rightarrow \pi^+\pi^-$ candidates are required to have an invariant mass between 462 and $534 \text{ MeV}/c^2$. A geometrical vertex fit with χ^2 probability above 0.1% is required, and the transverse flight distance from the event vertex must be greater than 0.2 cm .

\bar{D}^0 candidates are reconstructed in the decay channels $K^+\pi^-$, $K^+\pi^-\pi^0$, $K^+\pi^+\pi^-\pi^-$ and $K_s^0\pi^+\pi^-$ and D^- candidates in the decay channels $K^+\pi^-\pi^-$ and $K_s^0\pi^-$. Kaons from D^- decays and charged daughters from $\bar{D}^0 \rightarrow K^+\pi^-$ are required to have momenta greater than $200 \text{ MeV}/c$. All other charged \bar{D} daughters are required to have momenta greater than $150 \text{ MeV}/c$. For $\bar{D}^0 \rightarrow K^+\pi^-\pi^0$, we only reconstruct the dominant resonant mode, $\bar{D}^0 \rightarrow K^+\rho^-$, followed by $\rho^- \rightarrow \pi^-\pi^0$. The $\pi^-\pi^0$ mass is required to lie within $150 \text{ MeV}/c^2$ of the ρ mass [4] and the angle between the π^- and \bar{D}^0 in the ρ rest frame, $\theta_{D^0\pi}^*$, must satisfy $|\cos\theta_{D^0\pi}^*| > 0.4$. All \bar{D}^0 and D^- candidates are required to have a momentum greater than $1.3 \text{ GeV}/c$ in the $\Upsilon(4S)$ frame, an invariant mass within 3σ of the nominal value [4] and a geometrical vertex fit with a χ^2 probability greater than 0.1% . A mass constraint is applied to selected \bar{D} candidates.

Charged and neutral \bar{D}^* candidates are formed by combining a \bar{D}^0 with a π^- or π^0 . The momentum of the pion in the $\Upsilon(4S)$ frame is required to be less than $450 \text{ MeV}/c$. The soft π^- is constrained to originate from the beam spot when the D^{*-} vertex is fit. After the mass constraint to the \bar{D}^0 daughter, \bar{D}^* candidates with $m(\bar{D}^0\pi)$ within 2.5σ of the nominal mass [4] for D^{*-} , or within 4σ of the nominal mass [4] for \bar{D}^{*0} , are selected.

Candidates for leptonic decays of charmonium mesons must have at least one decay product positively identified as an electron or a muon. If it traverses the calorimeter, the second muon must be consistent with a minimum ionizing particle. J/ψ candidates are required to lie in the invariant mass interval 2.95 (3.06) to $3.14 \text{ GeV}/c^2$ for the e^+e^- ($\mu^+\mu^-$) channel. The e^+e^- ($\mu^+\mu^-$) invariant mass of $\psi(2S)$ candidates must be between 3.44 (3.64) and $3.74 \text{ GeV}/c^2$. A mass constraint is applied to selected candidates. $\psi(2S) \rightarrow J/\psi\pi^+\pi^-$ candidates are selected if the $\pi^+\pi^-$ mass is between 0.4 and $0.6 \text{ GeV}/c^2$ and the $\psi(2S)$ mass is within $15 \text{ MeV}/c^2$ of the nominal value [4]. All $\psi(2S)$ candidates must have momenta between 1.0 and $1.6 \text{ GeV}/c$ in the $\Upsilon(4S)$ rest frame.

B candidates are formed by combining a $\bar{D}^{(*)}$, J/ψ or $\psi(2S)$ candidate with a π^+ , ρ^+ , a_1^+ ($a_1^+ \rightarrow \pi^+\pi^-\pi^+$), K^{*0} ($K^{*0} \rightarrow K^+\pi^-$) or K^+ candidate that has a momentum larger than $500 \text{ MeV}/c$ in the $\Upsilon(4S)$ frame. For $B^0 \rightarrow D^{(*)-}\rho^+$, the π^0 from the ρ^+ decay must have an energy greater than 300 MeV . For $B^0 \rightarrow D^{(*)-}a_1^+$, the a_1^+ must have an invariant mass between 1.0 and $1.6 \text{ GeV}/c^2$, and the χ^2 probability of a vertex fit of the a_1^+ candidate

is required to be greater than 0.1% . Positive identification of kaons is required for modes with higher background, such as $B^+ \rightarrow \bar{D}^{*0}\pi^+$ with $\bar{D}^0 \rightarrow K^+\pi^+\pi^-\pi^-$.

Continuum $e^+e^- \rightarrow q\bar{q}$ background is rejected by requiring the normalized second Fox-Wolfram moment [6] for the event to be less than 0.5 . Further suppression is achieved by a mode-dependent restriction on the angle between the B_{rec} and B_{opp} thrust axes in the $\Upsilon(4S)$ frame.

B^0 and B^+ candidates are identified on the basis of the difference ΔE between the reconstructed energy and the beam energy $\sqrt{s}/2$ in the $\Upsilon(4S)$ frame, and the beam-energy substituted mass m_{ES} calculated from $\sqrt{s}/2$ and the reconstructed momentum of the candidate. B candidates are selected with $m_{\text{ES}} > 5.2 \text{ GeV}/c^2$ and $|\Delta E| < 3\sigma_{\Delta E}$, where $\sigma_{\Delta E}$ (10 to 30 MeV) is the measured resolution for each decay mode.

The decay position of the B_{rec} candidate is determined by requiring convergence of a vertex fit, where in addition the masses of the D mesons are constrained to their nominal values [4]. Precisions between 60 and $100 \mu\text{m}$ *rms* for the B_{rec} decay position in z and in the transverse plane are achieved, depending on the decay mode.

The vertex of the B_{opp} is determined from all tracks in the event after removing those associated with the B_{rec} candidate. Tracks from photon conversion candidates are rejected. Daughter tracks from K_s^0 or Λ candidates are replaced by the neutral parents. An additional constraint is imposed on the B_{opp} vertex using the B_{rec} vertex and three-momentum, the beam spot position, and the average $\Upsilon(4S)$ momentum. To reduce the bias in the forward z direction from charm decay tracks, the track with the largest contribution to the vertex χ^2 , if above 6 , is removed and the fit iterated until no track fails this requirement. Events are required to have at least 2 tracks remaining in the B_{opp} vertex, an error on Δz smaller than $400 \mu\text{m}$ and $|\Delta z| < 3000 \mu\text{m}$. The precision achieved on Δz , $190 \mu\text{m}$ *rms* on average, is dominated by the resolution on the B_{opp} vertex. A remaining bias of $-35 \mu\text{m}$ due to charm decays on the B_{opp} side is observed. We require $|\Delta t| < 18 \text{ ps}$ and find $6064 \pm 70 B^0$ and $6336 \pm 63 B^+$ signal events in a $\pm 2.5\sigma$ ($\sigma = 2.7 \text{ MeV}/c^2$ and $2.6 \text{ MeV}/c^2$, respectively) window around the m_{ES} peak above a small background ($\simeq 10\%$). The m_{ES} distributions for the final samples are shown in Fig. 1 along with the results of a fit with a Gaussian distribution for the signal and an ARGUS background function [7].

As already noted, the modeling of the resolution function \mathcal{R} is a crucial element of the B lifetime measurements. Studies with both Monte Carlo simulation and data show that the sum of a zero-mean Gaussian distribution and its convolution with a decay exponential provides a good trade-off between different sources of un-

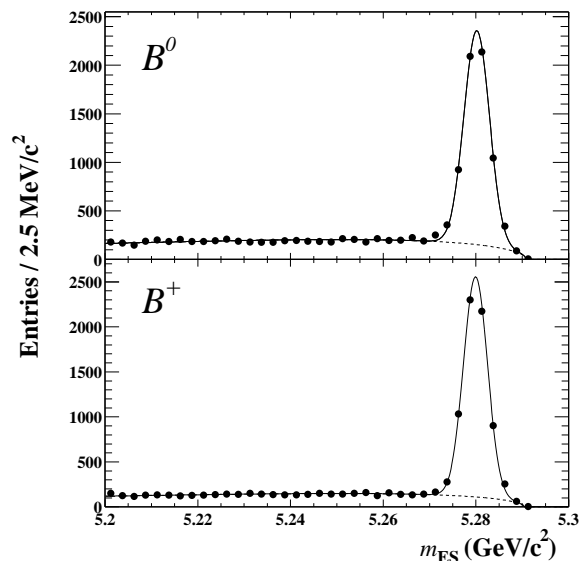


FIG. 1: m_{ES} distributions of the selected neutral (top) and charged (bottom) B_{rec} candidates.

certainties:

$$\mathcal{R}(\delta_t, \sigma | \hat{a} = \{h, s, \kappa\}) = h \frac{1}{\sqrt{2\pi}\sigma} \exp\left[-\frac{\delta_t^2}{2s^2\sigma^2}\right] + \int_{-\infty}^0 \frac{1-h}{\kappa\sigma} \exp\left[\frac{\delta'_t}{\kappa\sigma}\right] \frac{1}{\sqrt{2\pi}\sigma} \exp\left[-\frac{(\delta_t - \delta'_t)^2}{2s^2\sigma^2}\right] d(\delta'_t), \quad (3)$$

where δ_t is the difference between the measured and true Δt values. The model parameters \hat{a} are the fraction h in the core Gaussian component, a scale factor s for the per-event errors σ , and the factor κ in the effective time constant $\kappa\sigma$ of the exponential that accounts for the effect of charm decays. Monte Carlo studies show that the parameters \hat{a} obtained for different decay modes are compatible, as expected for Δt resolution dominated by the B_{opp} vertex. The resolution functions for B^0 and B^+ mesons differ slightly because the B_{opp} decays to a different admixture of D^- and \bar{D}^0 mesons. The difference is not significant given the present data sample size. Hence a single set of resolution function parameters is used for both B^0 and B^+ in the lifetime fits, and a small correction discussed later is applied to the results. While the resolution function \mathcal{R} describes almost all events, incorrectly measured *outlier* events are modeled separately as discussed below.

The unbinned maximum likelihood fit for the B lifetimes uses all events with $m_{ES} > 5.2 \text{ GeV}/c^2$. The probability p_i^{sig} for event i to be signal with Δt distribution \mathcal{G} , defined in Eq. 2, is estimated from the m_{ES} fit (Fig. 1) and the m_{ES} value of the B_{rec} candidate. Each event i then samples a PDF that includes signal, background, and outlier components:

$$\mathcal{F}(\Delta t_i, \sigma_i, p_i^{sig} | \tau; \hat{a}, \hat{b}, f_{out}^{sig}, f_{out}^{bkg}) = p_i^{sig} \cdot [(1 - f_{out}^{sig}) \cdot \mathcal{G}(\Delta t_i, \sigma_i | \tau, \hat{a}) + f_{out}^{sig} \cdot \mathcal{O}(\Delta t_i)] + (1 - p_i^{sig}) \cdot [(1 - f_{out}^{bkg}) \cdot \mathcal{B}(\Delta t_i | \hat{b}) + f_{out}^{bkg} \cdot \mathcal{O}(\Delta t_i)]. \quad (4)$$

The background Δt distribution, \mathcal{B} , for each B species is modeled by the sum of a prompt component and a lifetime component convoluted with a resolution function of the form given in Eq. 3, but with a separate set of parameters. The fraction of non-prompt background, its effective lifetime and the background resolution parameters are determined separately for charged and neutral B mesons. Signal and background outlier events have an assumed Δt behavior \mathcal{O} given by a Gaussian distribution with zero mean and a fixed 10 ps width. The fractions of outliers in signal and background are determined separately in the lifetime fit.

Since the same resolution function is used for neutral and charged B mesons, the fitting procedure maximizes the log-likelihood function $\ln \mathcal{L}$ formed from the sum of two terms, one for each B meson species, with common parameters \hat{a} for \mathcal{R} :

$$\ln \mathcal{L} = \sum_{i+} \ln[\mathcal{F}(\Delta t_{i+}, \sigma_{i+}, p_{i+}^{sig} | \tau_{B^+}; \hat{a}, \hat{b}_+, f_{out}^{sig,+}, f_{out}^{bkg,+})] + \sum_{i0} \ln[\mathcal{F}(\Delta t_{i0}, \sigma_{i0}, p_{i0}^{sig} | \tau_{B^0}; \hat{a}, \hat{b}_0, f_{out}^{sig,0}, f_{out}^{bkg,0})]. \quad (5)$$

The likelihood fit involves 19 free parameters. The parameter τ_{B^+} is replaced with $\tau_{B^+} = r \cdot \tau_{B^0}$ to estimate the statistical error on the lifetime ratio r . The lifetime values were kept hidden until the event selection and the Δt reconstruction method, as well as the fitting procedure, were finalized and the systematic errors were determined.

The fit results, after small corrections discussed below, are $\tau_{B^0} = 1.546 \pm 0.032 \text{ ps}$, $\tau_{B^+} = 1.673 \pm 0.032 \text{ ps}$ and $\tau_{B^+}/\tau_{B^0} = 1.082 \pm 0.026$, where the errors are statistical only. The resolution parameters \hat{a} ($h = 0.69 \pm 0.07$, $s = 1.21 \pm 0.07$ and $\kappa = 1.04 \pm 0.24$) are consistent with those found in a Monte Carlo simulation that includes detector alignment effects. The fitted outlier fractions in the B^+ and B^0 signals are both $0.2^{+0.3\%}_{-0.2\%}$. Figure 2 shows the results of the fit superimposed on the observed Δt distributions for B^0 and B^+ events within 2.5 standard deviations of the B mass in m_{ES} .

Table I summarizes the systematic uncertainties on the lifetime results. The full analysis chain, including event reconstruction and selection, has been tested with Monte Carlo simulation. The statistical precision on the consistency between the generated and fitted lifetimes is assigned as a systematic error. The resolution parameters \hat{a} are determined from the data by the fit, contributing $\pm 0.017 \text{ ps}$ in quadrature to the statistical error of the individual lifetime results. Thus, a large part of the Δt resolution uncertainty is included in the statistical error. Residual systematic uncertainties are attributed to limited flexibility of the resolution model. These contributions have been estimated by comparing results with different parametrizations. We correct our measurements for the small positive (negative) bias on the B^0 (B^+) lifetime due to differences in the Δt resolution functions for

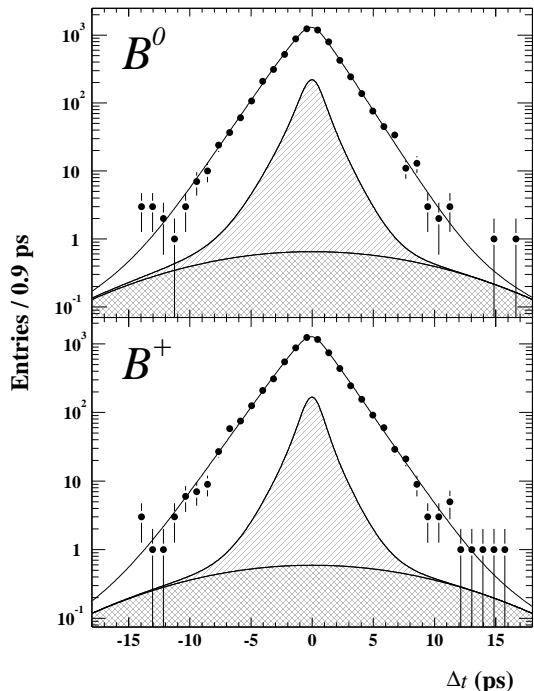


FIG. 2: Δt distribution for the B^0 (top) and B^+ (bottom) events within 2.5σ of the B mass in m_{ES} . The results of the fit are superimposed on the data. The single-hatched areas are the background components \mathcal{B} and the cross-hatched areas represent the outlier contributions. The probability of obtaining a lower likelihood, evaluated with a Monte Carlo technique, is 7.3%.

TABLE I: Summary of the systematic uncertainties.

Effect	$\delta(\tau_{B^0})$ (ps)	$\delta(\tau_{B^+})$ (ps)	$\delta(\tau_{B^+}/\tau_{B^0})$
MC statistics	0.009	0.007	0.006
\mathcal{R} parametrization	0.008	0.004	0.003
same \mathcal{R} for B^0 and B^+	0.004	0.005	0.006
Beam spot, $p_{B_{rec}}$	0.002	0.002	Cancels
Δt outliers	0.011	0.011	0.005
SVT alignment	0.008	0.008	Cancels
z scale	0.008	0.008	Cancels
Δz to Δt conversion	0.006	0.006	Cancels
Signal probability	0.003	0.003	0.003
Background modeling	0.005	0.011	0.005
Total in quadrature	0.022	0.023	0.012

B^0 and B^+ mesons arising from their decays to a different admixture of D^- and \bar{D}^0 mesons and estimated with a high-statistics Monte Carlo sample. The size of the correction is assigned as a systematic error. A small systematic error results from uncertainties on the beam spot position and vertical size, and the B_{rec} momentum vector, which are used to constrain the B_{opp} vertex. To estimate the systematic error due to the assumptions on the shape of the Δt outlier PDF, we first verified that the fitted lifetime results are stable when distributions wider than 10 ps or even flat are used in the fit. To investigate narrower shapes which are more signal-like, thousands of

experiments with sets of fixed values for the outlier width and mean were simulated and subjected to the nominal lifetime fit. The largest observed bias is taken as systematic uncertainty. Additional systematic uncertainties are due to the SVT alignment. The z length scale was determined to better than 0.5% from secondary interactions in a beam pipe section of known length. Approximations in the calculation of Δt from Δz and the uncertainty on the boost lead to small systematic errors. The errors on the m_{ES} fit parameters are used to determine the uncertainty on p^{sig} and the corresponding systematic error. The main systematic uncertainties related to backgrounds arise from changes in the background composition as a function of m_{ES} . An additional contribution arises from a 1-2% B^0 contamination of the B^+ signal sample and vice versa. We use Monte Carlo simulation to correct for these background effects and assign the sum in quadrature of the corrections as systematic uncertainty.

In summary, the B^0 and B^+ meson lifetimes and their ratio have been determined to be:

$$\begin{aligned}\tau_{B^0} &= 1.546 \pm 0.032 \text{ (stat)} \pm 0.022 \text{ (syst)} \text{ ps,} \\ \tau_{B^+} &= 1.673 \pm 0.032 \text{ (stat)} \pm 0.023 \text{ (syst)} \text{ ps, and} \\ \tau_{B^+}/\tau_{B^0} &= 1.082 \pm 0.026 \text{ (stat)} \pm 0.012 \text{ (syst)}.\end{aligned}$$

These are the most precise measurements to date, and they are consistent with the current world averages.

We are grateful for the extraordinary contributions of our PEP-II colleagues in achieving the excellent luminosity and machine conditions that have made this work possible. The collaborating institutions wish to thank SLAC for its support and the kind hospitality extended to them. This work is supported by DOE and NSF (USA), NSERC (Canada), IHEP (China), CEA and CNRS-IN2P3 (France), BMBF (Germany), INFN (Italy), NFR (Norway), MIST (Russia), and PPARC (United Kingdom). Individuals have received support from the Swiss NSF, A. P. Sloan Foundation, Research Corporation, and Alexander von Humboldt Foundation.

* Also with Università di Perugia, Perugia, Italy.

† Also with Università della Basilicata, Potenza, Italy.

- [1] I.I. Bigi, Nuovo Cim. **109A**, 713 (1996).
- [2] M. Neubert, C.T. Sachrajda, Nucl. Phys. **B483**, 339 (1997).
- [3] Throughout this paper, references to a hadron or to a decay reaction also imply their charge conjugate.
- [4] Particle Data Group, D.E. Groom *et al.*, Eur. Phys. J. **C15**, 1 (2000), and references therein.
- [5] BABAR Collaboration, B. Aubert *et al.*, hep-ex/0105044, to be published in Nucl. Instr. and Methods.
- [6] C.G. Fox, S. Wolfram, Nucl. Phys. **B149**, 413 (1979).
- [7] ARGUS Collaboration, H. Albrecht *et al.*, Z. Phys. **C48**, 543 (1990).